

Spectrum of 180° Bloch-type domain-wall excitations in yttrium iron garnet

A. V. Mikhailov

*L. D. Landau Institute for Theoretical Physics, Kosygina 2, Moscow 117 940, Russia
and Institute for Scientific Interchange Foundation, Torino, Italy*

I. A. Shimokhin

*L. D. Landau Institute for Theoretical Physics, Kosygina 2, Moscow 117 940, Russia
(Received 22 October 1991)*

The spectrum of excitations of a 180° domain wall in a cubic crystal with light uniaxial anisotropy is studied. Numerically, we have found high-frequency branches. The low-frequency (Goldstone) branch of excitations has a square-root long-wavelength singularity in almost all directions of the wave vector. For this branch our asymptotic long-wave expansion gives the angular dependence of the singular contribution.

I. INTRODUCTION

Here we present results of our numerical and analytical study of the excitation spectrum of a 180° domain wall in yttrium iron garnets (YIG). Samples that are made from YIG are widely used in experiments since they have extremely low dissipation of spin waves and a high Curie temperature. The effective anisotropy of YIG is quite small and therefore the dipole-dipole interaction becomes very important. There is a theory¹ that describes the dynamics of a domain wall in an external magnetic field if the anisotropy of a sample is strong enough (or if the so-called quality parameter $Q \gg 1$). A straightforward extrapolation of the results of that theory to the case of small anisotropy is obviously inconsistent and leads to disagreement with experimental data; in particular, the experimentally found group velocity of excitations propagating along the domain wall proved to be unexpectedly high.² YIG have a complicated crystal structure and the theory that has been recently developed for uniaxial anisotropy³ requires modification. Moreover, due to this structure new branches of the excitation spectrum do appear. Any nonlinear model that claims to describe the dynamics of domain walls should have a correct linear limit, i.e., demonstrate the true dispersion law corresponding to the excitation spectrum of a domain wall.

II. FORMULATION OF THE PROBLEM

The real crystallomagnetic structure of yttrium iron garnets is extremely complicated.^{1,4} In a typical experimental situation one can approximate it by a cubic crystal with a negative magnetocrystalline anisotropy coefficient and with the easy directions that lie along one of the cube diagonals. The uniaxial anisotropy could be due to other reasons like mechanical stress or the geometry of the sample and magnetostriction.

Thus we shall study the Landau-Lifshitz model with cubic and uniaxial anisotropy in the magnetostatic approximation:

$$\frac{1}{\gamma} \dot{\mathbf{M}} = \mathbf{M} \times \frac{\delta H}{\delta \mathbf{M}}, \quad \text{div}(\mathbf{H} + 4\pi\mathbf{M}) = 0, \quad \text{curl}\mathbf{H} = \mathbf{0}, \quad (1)$$

where \mathbf{M} is the magnetization vector, \mathbf{H} is the magnetic field, and γ is the gyromagnetic ratio. Here the Hamiltonian

$$H = \int (h_{\text{ex}} + h_a + h_{d-d}) dv$$

corresponds to the exchange, anisotropy, and dipole-dipole interactions:

$$h_{\text{ex}} = \frac{\alpha}{2M_s^2} \sum_{i=1}^3 \left(\frac{\partial \mathbf{M}}{\partial x_i} \right)^2,$$

$$h_a = \frac{K_1}{M_s^4} (M_1^2 M_2^2 + M_2^2 M_3^2 + M_3^2 M_1^2) + \frac{\tau |K_1|}{12} \left(1 - \frac{(\mathbf{M} \cdot \mathbf{n})^2}{M_s^2} \right),$$

$$h_{d-d} = -\frac{1}{2} (\mathbf{M} \cdot \mathbf{H}),$$

where M_s is the saturation magnetization ($M^2 = M_s^2$), α is the exchange constant, K_1 is the cubic anisotropy constant, and the constant τ characterizes the uniaxial anisotropy along the unit vector \mathbf{n} . More accurate accounting of the magnetoelastic interaction slightly modifies coefficients in h_a [see Refs. (5-7)] but does not affect the following consideration much.

Let $\mathbf{n} = (1, 1, 1)/\sqrt{3}$ and the normal vector to the Bloch-type domain wall is assumed to be parallel to $[0, 1, \bar{1}]$. It is convenient to make an orthogonal change of coordinates and a rescaling to introduce the unit length vector field \mathbf{S} , $\mathbf{S}^2 = 1$ instead of \mathbf{M} :

$$M_1 = M_s \left(-\frac{2}{\sqrt{6}} S_1 + \frac{1}{\sqrt{3}} S_3 \right),$$

$$M_2 = M_s \left(\frac{1}{\sqrt{6}} S_1 - \frac{1}{\sqrt{2}} S_2 + \frac{1}{\sqrt{3}} S_3 \right),$$

$$M_3 = M_s \left(\frac{1}{\sqrt{6}} S_1 + \frac{1}{\sqrt{2}} S_2 + \frac{1}{\sqrt{3}} S_3 \right)$$

[in new coordinates the vector $\mathbf{n} = (0, 0, 1)$]. The anisotropy contribution in the Hamiltonian in the new variables is

$$h_a = \frac{|K_1|}{12} [3S_1^4 + 4S_3^4 + 4\sqrt{2}S_1^3S_3 + 6S_1^2S_2^2 - 12\sqrt{2}S_1S_2^2S_3 + \tau(1 - S_3^2)].$$

The form of the other contributions is obvious.

An exact solution of Eqs. (1) that depends on one spatial coordinate y and corresponds to the Bloch-type domain wall has been found by Lilley.⁸ In terms of \mathbf{S} and \mathbf{H} it can be rewritten as

$$\mathbf{S}^0 = \left(\frac{1}{\sqrt{1 + \Delta(by)^2}}, 0, \frac{\Delta(by)}{\sqrt{1 + \Delta(by)^2}} \right), \quad \mathbf{H}^0 = \mathbf{0}, \quad (2)$$

where

$$a = \frac{\sqrt{\tau^2 + 9\tau}}{8 + \tau}, \quad b = \sqrt{\frac{|K_1|(8 + \tau)}{12\alpha}}, \quad c = \frac{2\sqrt{2}}{8 + \tau}$$

and

$$\Delta(by) = a \sinh(by) + c.$$

For small τ the 180° domain wall (2) (see Fig. 1) is a combination of two domain walls of $\sim 71^\circ$ and $\sim 109^\circ$ separated by a distance of about

$$\delta y \approx \frac{1}{b} \sinh^{-1} \left(\frac{3\sqrt{2}}{4a} \right) \approx \sqrt{\frac{3\alpha}{2|K_1|}} \ln \frac{1}{\tau}.$$

A pure uniaxial anisotropy model can be obtained from the above as a limit when $\tau \rightarrow \infty$, $|K_1| \rightarrow 0$, $\tau|K_1|/12 \rightarrow$

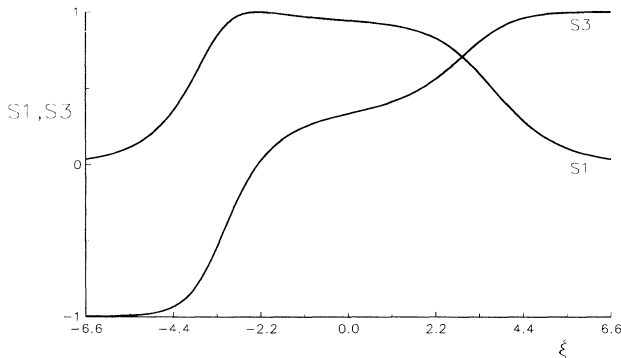


FIG. 1. Typical shape of a Bloch-type domain wall ($S_2 = 0$) corresponding to solution (2) with $\tau = 3.8 \times 10^{-2}$. One can see $\sim 109^\circ$ and $\sim 79^\circ$ subdomains.

β ; that means that

$$a \rightarrow 1, \quad b \rightarrow \sqrt{\beta/\alpha}, \quad c \rightarrow 0. \quad (3)$$

In this limit solution (2) turns into the well-known Bloch solution of the uniaxial model.

To study small excitations of the domain wall we linearize Eqs. (1) near the exact solution (2). Thus we represent \mathbf{S} and \mathbf{H} in the form

$$\mathbf{S} = \mathbf{S}^0 + \mathbf{s}, \quad |\mathbf{s}| \ll 1, \quad \mathbf{H} = M_s \text{div} \phi.$$

Linearizing $\mathbf{S}^2 = 1$, we get $(\mathbf{S}^0 \cdot \mathbf{s}) = 0$, therefore the three-component vector field \mathbf{s} can be parametrized by two functions. Then we separate variables assuming that \mathbf{s} and ϕ are plane waves with wave vector $\kappa = (\kappa_x, \kappa_z)$ and frequency Ω and introduce dimensionless variables:

$$\begin{aligned} s_x &= S_3^0 \Phi(\xi) \cos(\kappa_x x + \kappa_z z - \Omega t), \\ s_y &= \Psi(\xi) \sin(\kappa_x x + \kappa_z z - \Omega t), \\ -s_z &= S_1^0 \Phi(\xi) \cos(\kappa_x x + \kappa_z z - \Omega t), \\ \phi &= 2\alpha b f(\xi) \sin(\kappa_x x + \kappa_z z - \Omega t), \end{aligned}$$

$$\Omega = \frac{2\gamma\alpha b^2}{M_s} \omega, \quad \kappa_x = \eta b \sin \vartheta, \quad \kappa_z = \eta b \cos \vartheta, \quad y = \frac{\xi}{b}.$$

Functions Φ and Ψ characterize the deviation of \mathbf{S} in the plain of the domain wall and across it, respectively. In these variables the linearized equations have the form

$$\begin{aligned} D_1 \Phi &= \omega \Psi - \eta T(\xi, \vartheta) f, \\ D_2 \Psi &= \omega \Phi + f', \\ f'' - \eta^2 f &= \frac{1}{Q} [\Psi' + \eta T(\xi, \vartheta) \Phi], \end{aligned} \quad (4)$$

where

$$Q = \frac{(8 + \tau)|K_1|}{24\pi M_s^2}, \quad T(\xi, \vartheta) = \frac{\cos \vartheta - \sin \vartheta \Delta(\xi)}{\sqrt{1 + \Delta(\xi)^2}}$$

and the differential operators D_1 and D_2 are of the form

$$\begin{aligned} D_1 &= \frac{d^2}{d\xi^2} - \left(1 + \eta^2 - \frac{6(a^2 + c^2 - 1) - 2 - 6c\Delta(\xi)}{1 + \Delta(\xi)^2} \right. \\ &\quad \left. + \frac{16c\Delta(\xi) - 8(a^2 + c^2 - 1)}{(1 + \Delta(\xi)^2)^2} \right), \\ D_2 &= \frac{d^2}{d\xi^2} - \left(1 + \eta^2 - \frac{2(a^2 + c^2 - 1) - 2 + 6c\Delta(\xi)}{1 + \Delta(\xi)^2} \right. \\ &\quad \left. + \frac{6c\Delta(\xi) - 3(a^2 + c^2 - 1)}{(1 + \Delta(\xi)^2)^2} \right). \end{aligned}$$

Now the problem of finding the excitation spectrum of the domain wall can be formulated in the following way: in three-dimensional space with coordinates $(\eta, \vartheta, \omega)$ one has to find a set of points such that the system of equations (5) possesses a solution vanishing with $\xi \rightarrow \pm\infty$. This set is nothing but the dispersion law of the linear excitations of the domain wall. It depends on the parameters Q and τ .

The excitation spectrum of a domain wall represents a set of sheets located within a band forbidden for space volume spin waves:

$$\omega^2 < (1 + \eta^2)[1 + \eta^2 + (\sin \vartheta)^2/Q].$$

In the case of the uniaxial anisotropy, the spectrum is invariant (see Ref. 3) with respect to the complete reflection

$$\kappa \rightarrow -\kappa, \quad \Omega \rightarrow -\Omega \quad (5)$$

and the reflection with respect to the x axis $\kappa_x \rightarrow \kappa_x$, $\kappa_z \rightarrow -\kappa_z$, $\Omega \rightarrow \Omega$. In the case under consideration we obviously have (5) but there is no last symmetry which exists in the uniaxial case due to an extra symmetry of the domain wall. There is no mathematical reason to expect invariance of the spectrum with respect to the usual spatial reflection $\kappa \rightarrow -\kappa$, $\Omega \rightarrow \Omega$.

III. LONG-WAVELENGTH ASYMPTOTE OF THE-LOW FREQUENCY BRANCH

The method that we use here is rather similar to the one that we have developed for the case of the uniaxial anisotropy.³ But the problem under consideration is much more complicated and we have to assume $Q \ll 1$ to obtain the main contribution in the long-wavelength asymptote of the low-frequency branch of the spectrum.

If the $\eta = 0$ system of equations (4) has an exact solution,

$$\omega = 0, \quad \Phi_0 = \frac{A_0 \cosh(\xi)}{1 + \Delta(\xi)^2}, \quad \Psi_0 = 0, \quad f_0 = 0, \quad (6)$$

which corresponds to the "shift" mode. If ξ goes to $\pm\infty$ all of the coefficients of Eqs. (4) become constant and any solution turns into a superposition of exponents which,

for small η and ω , are of the form

$$\exp(\pm\eta\mu\xi), \quad \exp(\pm\xi), \quad \exp(\pm\xi/\sqrt{Q}), \quad (7)$$

where

$$\mu = \sqrt{\frac{Q + \sin \vartheta}{Q + 1}}.$$

Like the uniaxial case here we are looking for the asymptotic expansion of the vector eigenfunction (Φ, Ψ) and eigenvalue ω of the form

$$\begin{aligned} \omega &= \sqrt{\eta}\omega_1 + \eta\omega_2 + o(\eta), \\ \Phi &= \Phi_0 + \eta\Phi_1 + o(\eta), \\ \Psi &= \sqrt{\eta}\Psi_1 + \eta\Psi_2 + o(\eta), \end{aligned} \quad (8)$$

where Φ_1 , Ψ_1 , and Ψ_2 are supposed to be exponentially vanishing if $\xi \rightarrow \pm\infty$. In order to determine this expansion we move to the eigenvalue problem for an integral-differential operator. Using the Green function

$$G(\xi - \zeta) = -\frac{1}{2\eta} \exp(-\eta|\xi - \zeta|), \quad G_{\xi\xi} - \eta^2 G = \delta(\xi - \zeta),$$

one can formally solve the last equation in system (4):

$$f = -\frac{1}{2Q} \int_{-\infty}^{+\infty} e^{-\eta|\xi - \zeta|} \left(\frac{\cos \vartheta - \sin \vartheta \Delta(\zeta)}{\sqrt{1 + \Delta(\zeta)^2}} \Phi(\zeta) - \operatorname{sgn}(\xi - \zeta) \Psi(\zeta) \right) d\zeta. \quad (9)$$

Now it follows from (4) that

$$D_1 \Phi = \omega \Psi + \frac{\eta}{2Q} \int_{-\infty}^{+\infty} e^{-\eta|\xi - \zeta|} [T(\zeta, \vartheta) \Phi(\zeta) - \operatorname{sgn}(\xi - \zeta) \Psi(\zeta)] d\zeta, \quad (10)$$

$$D_2 \Psi = \omega \Phi + \frac{1}{Q} \Psi + \frac{\eta}{2Q} \int_{-\infty}^{+\infty} e^{-\eta|\xi - \zeta|} [\operatorname{sgn}(\xi - \zeta) T(\zeta, \vartheta) \Phi(\zeta) - \Psi(\zeta)] d\zeta. \quad (11)$$

Substituting expansion (8) in (10) and (11) and equating terms at each power of η , we obtain an approximate ansatz for Φ_1 , Ψ_1 , and Ψ_2 . Namely,

$$\Phi_1 = A_1 \frac{\Delta(\xi)}{\sqrt{1 + \Delta(\xi)^2}} e^{-\mu\eta|\xi|} + \tilde{\Phi}_1, \quad (12)$$

$$\Psi_2 = B_2 \frac{\Delta(\xi)}{\sqrt{1 + \Delta(\xi)^2}} e^{-\mu\eta|\xi|} + \tilde{\Psi}_2, \quad (13)$$

where A_1 and B_2 do not depend on ξ and Ψ_1 , $\tilde{\Phi}_1$, and $\tilde{\Psi}_2$ are functions vanishing at $\xi \rightarrow \infty$ as $e^{-|\xi|}$. Now it follows from (8) and (10)–(13) that

$$D_1 \Phi_1 = \omega_1 \Psi_1 + \frac{1}{2Q} T(\xi, \vartheta) I_1, \quad (14)$$

$$D_2 \Psi_1 = \frac{1}{Q} \Psi_1 + \omega_1 \Phi_0, \quad (15)$$

$$D_2 \Psi_2 = \frac{1}{Q} \Psi_2 + \omega_2 \Phi_0 + \frac{1}{2Q} I_2, \quad (16)$$

where

$$I_1 = \frac{2 \cos \vartheta A_0}{a} - \frac{2 \sin \vartheta A_1}{1 + \mu} + \frac{2 B_2}{1 + \mu}, \quad (17)$$

$$I_2 = \frac{2 \cos \vartheta A_0 \Delta(\xi)}{a \sqrt{1 + \Delta(\xi)^2}} + \frac{2 \sin \vartheta A_0}{a \sqrt{1 + \Delta(\xi)^2}}. \quad (18)$$

There are two contributions in (14) and (16), namely, a slow decaying part with exponential rate $\exp(-\eta\mu|\xi|)$ and a fast decaying one which vanishes as $\exp(-\xi)$. Collecting the coefficients of the slow exponents we get the following linear equations:

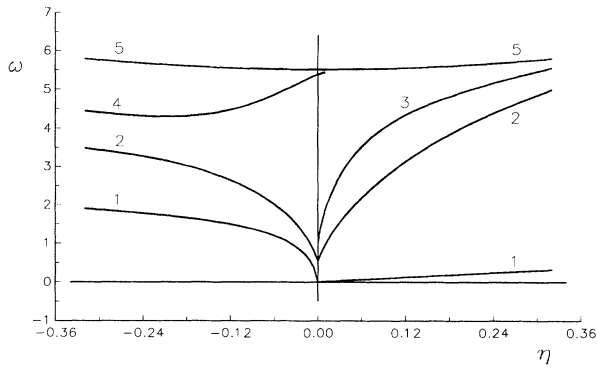


FIG. 2. The excitation spectrum for $\vartheta = \pm\pi/2$. Curves 1–4 correspond to different branches and 5 is the bottom of the space volume spin wave zone.

$$A_1 - \frac{\sin(\vartheta)}{Q} \left(\frac{\cos(\vartheta)}{a} A_0 - \frac{\sin(\vartheta)}{1 + \mu} A_1 + \frac{1}{1 + \mu} B_2 \right) = 0, \quad (19)$$

$$\left(1 + \frac{1}{Q} \right) B_2 + \frac{1}{Q} \frac{\cos(\vartheta) A_0}{a} = 0 \quad (20)$$

for coefficients A_1 and B_2 . Their solution gives

$$A_1 = \frac{\sin \vartheta \cos \vartheta}{a(1 + Q)\mu} A_0, \quad B_2 = -\frac{\cos \vartheta}{a(1 + Q)} A_0. \quad (21)$$

In the uniaxial case we have succeeded in solving the fast decaying part of equations corresponding to (14) and (15) exactly and found ω_1 for any Q . In the present case we have not managed to find the solution in a closed form, but if Q is small enough we can present the solution Ψ_1 in the form of a series

$$\Psi_1 = -Q\omega_1 A_0 \sum_{n=0}^{\infty} (QD_2)^n \frac{\cosh(\xi)}{1 + \Delta(\xi)^2},$$

or even restrict ourselves with the first term only:

$$\Psi_1 = -Q\omega_1 A_0 \frac{\cosh(\xi)}{1 + \Delta(\xi)^2} + O(Q^2). \quad (22)$$

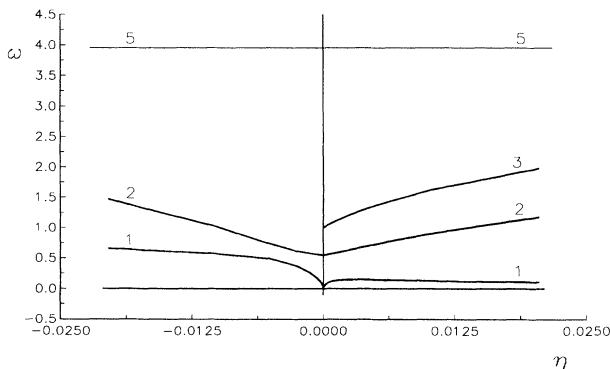


FIG. 3. The excitation spectrum for $\vartheta = \pi/4, 5\pi/4$.

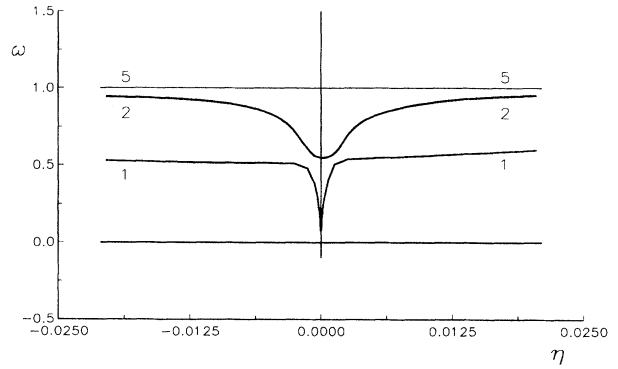


FIG. 4. The excitation spectrum for $\vartheta = 0, \pi$.

Now to determine ω_1 we consider the solvability condition of (14). Let us multiply Eq. (14) on Φ_0 and integrate the result over ξ from $-\infty$ to ∞ . The left-hand side vanishes because the operator D_1 is self-adjoint and $D_1\Phi_0 = 0$. The right-hand side gives us the equation for ω_1

$$Q\omega_1^2 A_0 \sum_{n=0}^{\infty} Q^n J_n = \frac{I_1}{2Q} \int_{-\infty}^{+\infty} \frac{\cosh(\xi) T(\xi, \vartheta)}{1 + \Delta(\xi)^2} d\xi, \quad (23)$$

where

$$J_n = \int_{-\infty}^{+\infty} \frac{\cosh(\xi)}{1 + \Delta(\xi)^2} D_2^n \frac{\cosh(\xi)}{1 + \Delta(\xi)^2} d\xi.$$

It follows from (17) and (21) that

$$I_1 = \frac{2A_0 Q \cos \vartheta}{a \sqrt{(1 + Q)[Q + (\sin \vartheta)^2]}}.$$

The last integral in (23) can be easily evaluated and finally the right-hand side of (23) takes the form

$$\frac{2A_0 (\cos \vartheta)^2}{a^2 \sqrt{(1 + Q)[Q + (\sin \vartheta)^2]}}.$$

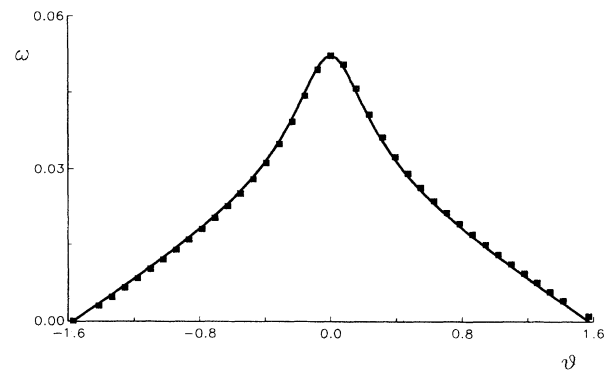


FIG. 5. Angular dependence of the frequency in the Goldstone branch 1. The solid line corresponds to (24), blocks are numerical results. Here $Q = 3.4 \times 10^{-2}$, $\tau = 3.84 \times 10^{-2}$, $\eta = 10^{-5}$.

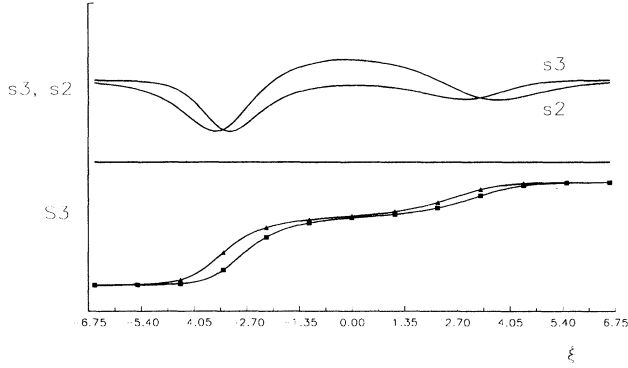


FIG. 6. The bend Goldstone mode (branch 1, $\vartheta = \pi/2$). On the upper part s_2 and s_3 are eigenfunctions corresponding to deviations of vector \mathbf{S}^0 . On the bottom part: Two opposite phases of oscillation of S_3 .

On the left-hand side of (23) each integration can be, in principle, evaluated in elementary functions. For small Q we shall keep the first term

$$J_0 = \int_{-\infty}^{+\infty} \frac{\cosh(\xi)^2}{\{1 + [a \sinh(\xi) + c]^2\}^2} d\xi.$$

This quadrature can be evaluated in elementary functions but we have not found a compact form for the result. If a is small (as in the case of yttrium iron garnets) one can expand J_0 :

$$J_0 = \frac{1}{a^2} [1 + c \tan^{-1}(c)] + O(1) \text{ if } a \rightarrow 0.$$

Thus for $Q \ll 1$ and any ϑ we have

$$\omega = \sqrt{\eta} \frac{\sqrt{2} |\cos \vartheta|}{aQ^{1/2} [Q + (\sin \vartheta)^2]^{1/4} J_0^{1/2}} + O(\eta). \quad (24)$$

The result obtained perfectly matches with the one for the uniaxial case (see Ref. 3) if $Q \rightarrow 0$ and $\tau \rightarrow \infty$.

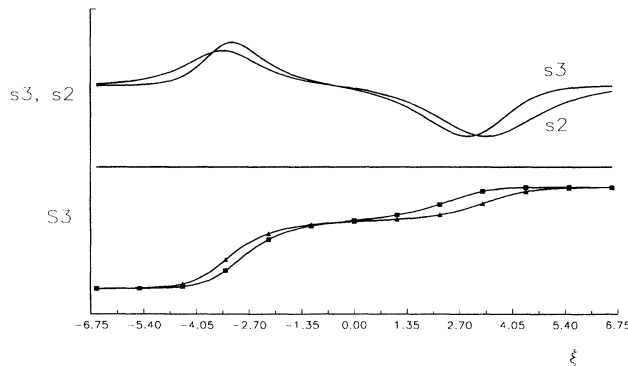


FIG. 7. The width oscillating mode (branch 2, $\vartheta = \pi/2$).

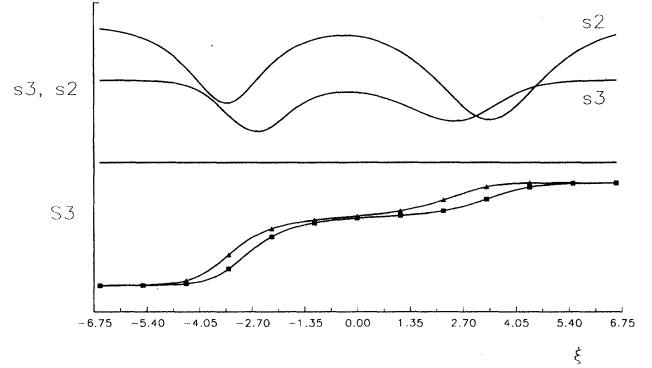


FIG. 8. The Gilinskii mode (branch 3, $\vartheta = \pi/2$).

IV. DISCUSSION OF NUMERICAL RESULTS

We have been studying the spectrum of excitations numerically for the parameters $Q = 3.4 \times 10^{-2}$ and $\tau = 3.8 \times 10^{-2}$ that experimentalists usually use to describe the yttrium iron garnet.⁹ In the most interesting long-wavelength region we have found four branches of the spectrum (see Fig. 2). We remind the reader that in the case of uniaxial anisotropy there are two branches only, namely, the low-frequency branch and the Gilinskii branch.³

The low-frequency branch corresponds to a bend Goldstone mode (see Figs. 2–4, branch 1). Due to the dipole-dipole interaction it has a square root singularity at $\eta \rightarrow 0$ in all directions (except for $\vartheta = \pm\pi/2$ where it has linear behavior). Our asymptotical result (24) perfectly coincides with the computer simulation at small η (see Fig. 5). In particular, this means that the group velocity $\mathbf{v}_{\text{gr}} = \text{grad}_{\eta} \omega$ becomes very high at low values of η (and can in principle violate the applicability of the magnetostatic approximation). In the real experiments² an anomalously high velocity of propagation of pulses along a domain wall in the direction $\vartheta = 0$ has been observed. Eigenfunctions s_2 and s_3 , corresponding to the deviation of the vector \mathbf{S}^0 in this mode are shown in Fig. 6. Two different phases of oscillation of the component S_3 are shown in the bottom part of Fig. 6.

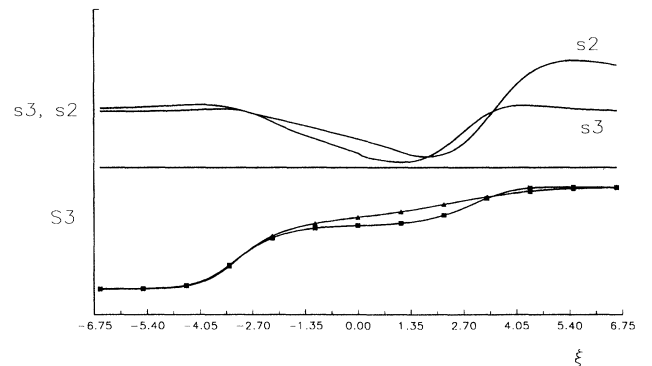


FIG. 9. New mode (branch 4, $\vartheta = \pi/2$).

Branch 2 in Figs. 2–4 has a gap and corresponds to oscillations of the width of a domain wall. In Fig. 7 one can see that the 109° and 79° subdomains are moving in opposite phases. This mode resembles the one that exists in the simple mechanical model of two weakly interacting strings. It does not exist in uniaxial ferromagnets. There was an attempt to find the gap of the spectrum at $\eta = 0$ theoretically.¹⁰ Unfortunately the result obtained is not in good agreement with our computer simulation. Our analysis has shown that the theoretical construction in Ref. 10 had been based on a wrong assumption. Namely, the author has neglected the contribution of the fast exponents $\exp(-|\xi|/\sqrt{Q})$ that become important for the finite gap modes (contrary to the Goldstone one). Our computed eigenfunction does not fit the assumption which had been made in Ref. 10.

Branch 3 exists if $0 < \vartheta < \pi$. It corresponds to the Gilinskii branch in the uniaxial case.^{11,3} Gilinskii had

found it at $\vartheta = \pi/2$, the angular dependency has been recently described in Ref. 12. Here we do not see a big difference with the uniaxial case. One can imagine the oscillations with the help of Fig. 8.

Branch 4 exists in a narrow region of angles $\vartheta \sim \pi/2$ when the spin wave gap is high enough. It seems that this branch has been unknown. In Fig. 9 the eigenfunctions and deformations of the domain wall at different phases of oscillation are shown.

ACKNOWLEDGMENTS

We thank Dr. V. Synogach for numerous discussions of present experiments and bibliography. One of us (A.M.) would like to thank the ISI Foundation for support and hospitality.

-
- ¹ A. P. Malozemoff and J. C. Slonczewski, *Magnetic Domain Walls in Bubble Materials* (Academic, New York, 1979).
² V. S. Gornakov, L. M. Dedukh, V. I. Nikitenko, and V. T. Synogach, *Zh. Eksp. Teor. Fiz.* **90**, 2090 (1986).
³ A. V. Mikhailov and I. A. Shimokhin, *Zh. Eksp. Teor. Fiz.* **97**, 1966 (1990).
⁴ I. V. Kolokolov, V. S. L'vov, and V. B. Cherepanov, *Zh. Eksp. Teor. Fiz.* **84**, 1043 (1983).
⁵ G. Rieder, *Abha. Braunsch. Wiss. Ges.* **11**, 20 (1959).
⁶ W. Döring, *Handbook of Physics* (Springer, Berlin, 1966),

- Bd. 18/2.
⁷ A. Hubert, *Theorie Der Domanenwande in Geordnetem Medien* (Springer-Verlag, Berlin, 1974).
⁸ B. A. Lilley, *Philos. Mag.* **41**, 792 (1950).
⁹ L. M. Dedukh, V. I. Nikitenko, and V. T. Synogach, *Zh. Eksp. Teor. Fiz.* **94**, 312 (1988).
¹⁰ H. E. Khodenkov, *Solid State Phys.* **31**, 226 (1989).
¹¹ I. A. Gilinskii, *Zh. Eksp. Teor. Fiz.* **68**, 1032 (1975).
¹² I. A. Shimokhin, *Phys. Stat. Solidi B* **167**, 243 (1991).